High Precision Encoders for GEO Space Applications

Martin Reinhardt, Konrad Panzlaff,
Karl-Georg Friederich, Frank Heine, Roland Himmler, Klaus Maier, Eberhard Möss
Tesat Spacecom
Backnang, Germany

Clive Parker, Simon McAdam, Jason Slack, Colin Howley
Renishaw
Wotton-under-Edge, United Kingdom

Rolf Meyer
DLR
Bonn, Germany

Abstract— **High precision encoders are used by earth observation instruments and in mechanisms for Laser Communication Terminals. Together with Renishaw, Tesat Spacecom has developed and tested a micro-radian resolution encoder for the Laser Communication Terminal (LCT), designed for precision pointing applications especially in GEO environments with 15 years lifetime and in high duty cycle applications. The encoders will be used for the LCTs on the Sentinel 1A and EDRS A and C LCTs. The design principles, performance parameters and the test campaign will be presented.**

Keywords: encoder; optical communication; mechanisms

I. INTRODUCTION

The encoder described herein is an optical angular encoder. Basically, the encoder is relative, but embedded reference marks guarantee that the absolute position is initialized to the full accuracy and repeatability of the relative count over the entire lifetime. As multiple and distinguishable reference marks are embedded in the scale, a few degrees of movement are sufficient for initialization independently from the starting position.

Electronic parts, mechanical design and processes are chosen to be inherently suitable for GEO space application, while the basic principles are entirely taken-over from commercial optical encoders developed and manufactured by Renishaw. Intellectual property and patents from Renishaw are licensed to Tesat.

On the one hand, the objective of the development was to reproduce the performance of the commercial encoder; on the other hand full compatibility to specific space demands like the radiation impact of a GEO orbit and harsh thermal and vibration loads was aimed for. Both performance and space specific requirements were achieved to the full extent.

Fig. 1 shows the location of two optical encoders in a Laser Communication Terminal (LCT) outside the spacecraft.

Following a short specification of the encoder in chapter II, the basic principle of operation is explained in chapter III. In chapter IV, the design is described. In chapter V "Performance and Function Tests", emphasis is placed on the most crucial performance criterion, the position jitter. Test set-up and jitter measurement results versus frequency are discussed in detail. Space specific environmental tests and the qualification status are the subject of chapter VI. While analysis show full compliance to the environmental requirements, the environmental tests have already been executed to flight model (FM) level. The qualification on part level has successfully finished. The qualification tests on an entire read-head are ongoing.

II. SPECIFICATION

A brief summary of the encoder specification is given:

- Scale diameter 178 mm

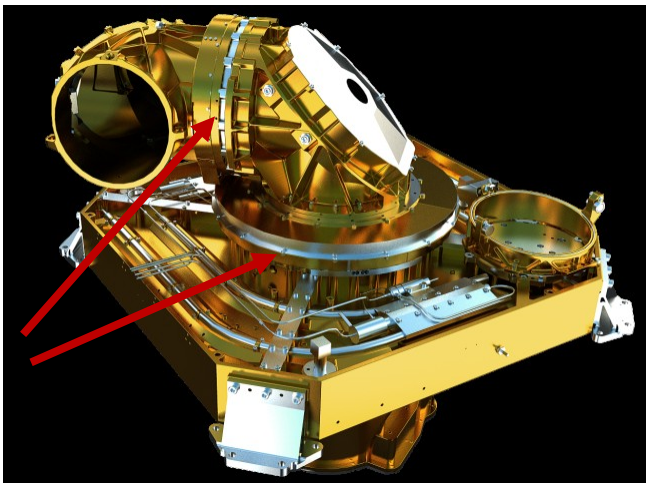

Figure 1. Location of angular encoders in a Laser Communication Terminal

Copyright (c) ICSOS 2012. All Rights Reserved.

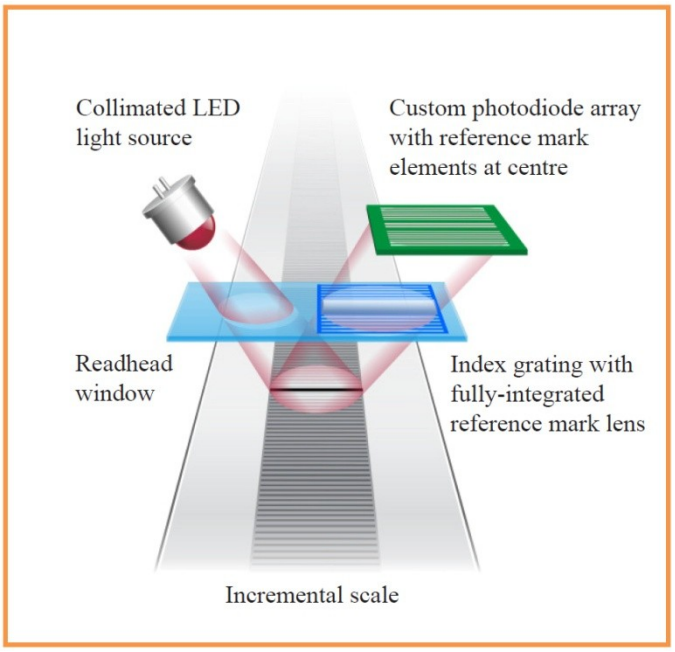

Figure 2. Encoder principle of operation

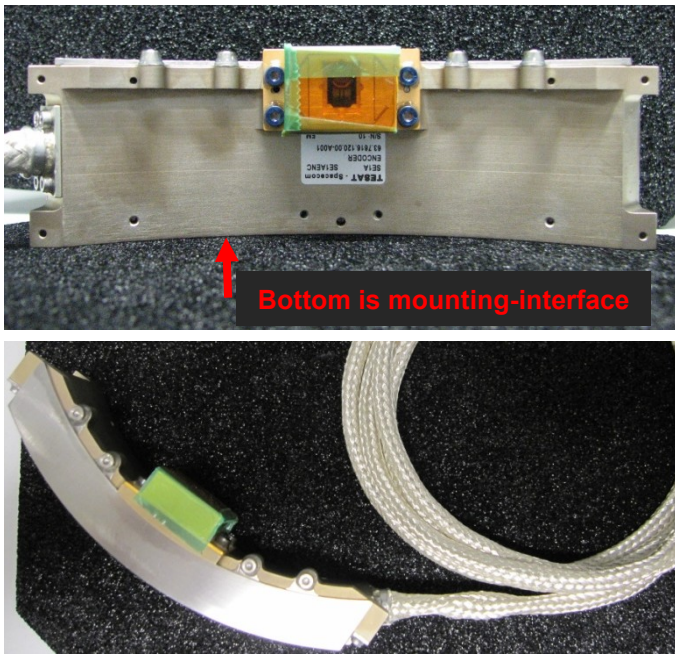

Figure 3. Photos of the encoder read-head with cable assembly (green tape is for protection)

- Resolution < 0.5 µrad
- Position jitter < 1 µrad rms over 1° range and $f < 100$ Hz (interpolation error < 0.5 µrad rms)
- Velocity > 25°/s
- Electric power < 3 W
- Mass < 300 g without scale
- Temperature $-30°C \leq T \leq +70°C$ (operating and storage nominal)
- Vibration Design 150 g static, random 24.7 g rms
- Radiation GEO and LEO orbit 15 years
- EMC Radiated according to MIL-STD-461/462, emission 10 dB below MIL-STD-461/462 E
- Lifetime 15 years in GEO orbit

III. Principle of Operation

The encoder principles are closely related to Renishaw's optical incremental rotary encoder series TONiC™.

A. Incremental Path

As illustrated in Fig. 2, a collimated beam illuminates the scale. The light is emitted by an infrared LED at the wavelength of 850 nm. On the scale, marks and spaces with a period of 20 µm and a mark-to-space ratio of 50 % are engraved. Light is reflected from the scale as a set of diffraction orders. These orders are then incident on a phase diffraction grating (optimised to produce no zero'th order) producing more diffraction orders. The orders from the scale and index interfere at the detector plane to produce a set of interference fringes. As the light source is partially coherent, only orders with small path length differences interfere. The result is an interference fringe that is substantially sinusoidal and free from harmonics. It is technically standard to manufacture an optical grating with the optical performance necessary for precise diffraction whereas in the optical scheme designed by Renishaw, the scale needs not to have such a high optical quality, as the configuration filters out unwanted energy. The detected electrical signals are very precise sine and cosine signals. These signals are amplified, combined and A/D converted. In the digital domain, interpolation takes place, increasing the resolution by a factor of e.g. 512, leading to a resolution of approximately 40 nm. (Higher interpolation factors are also standard for Renishaw's commercial encoders.)

With a scale diameter of 178 mm, nearly 15 bit can be achieved without interpolation. By interpolation the range is increased by 9 bit to nearly 24 bit.

The illuminated spot size on the scale is > 3 mm. More than 100 periods with 20 µm length are sampled in parallel forming the average of the illuminated area. The advantage of this method is: If there are scratches or dirt on the scale, the resulting signal will decrease a little bit in contrast, but not in quality in terms of being sinusoidal, which is necessary for precise interpolation. The immunity against single lines being absent can even be used to embed reference marks in the scale.

This design principle of Renishaw encoders makes them tolerant to scale degradation, misalignment and other degradation mechanisms.

B. Reference Marks

In order to obtain a reference mark, which is aligned perfectly to the incremental line pattern, several periods are made completely black. The black mark is detected by special

Copyright (c) ICSOS 2012. All Rights Reserved.

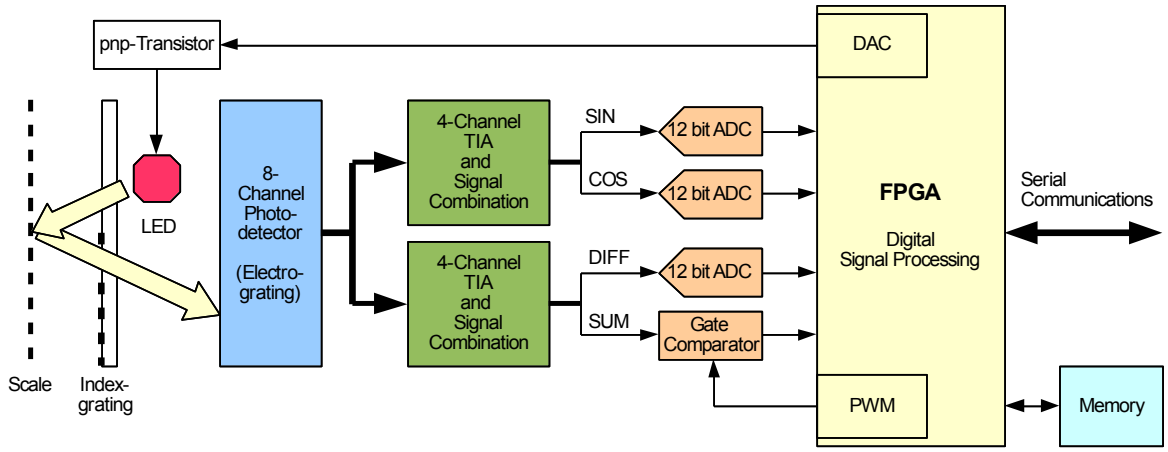

Figure 4. Encoder read-head block diagram

segments of the photodiode array as a triangular light drop pulse. The optical imaging is done by a Fresnel zone plate, embedded in the optical grating.

Multiple reference marks are placed along the scale. The distance between two marks is varied. Each distance is unique along the scale, therefore coding the absolute position. On a scale diameter of 178 mm, there are 184 embedded reference marks. The distance which has to be passed in order to detect two adjacent reference marks, is $360°/92 = 3.9°$ in the worst case. The incremental encoder has become quasi-absolute with a calibration distance of 3.9°.

C. *Scale*

The scale is usually the movable part of the encoder system. It is placed on the rotor of the drive system. Stainless steel is the material. Mark size is 10 µm wide and 5.5 mm long. The reflectivity of the marks is < 10 %. The long range encoder error is dominated by geometrical errors of the scale. The scale can be either a ring, which is assembled to the rotor of the drive system, or the scale pattern can be directly written to the rotary part of the bearing assembly. The latter method eliminates mounting tolerances of the ring and significantly reduces mass and volume.

IV. DESIGN

A. *Mechanics*

The size and form of the encoder housing is adapted to the available volume around the bearing system. The housing is curved, see Fig. 3. For mounting, four threaded holes are on the lower small edge. A pigtail is used for electrical connection. The electro-optics and optics are arranged in a separate so called "optical module" (golden in Fig. 3). This housing is a Kovar™ package with glass sealed feed through pins, an arrangement, which supports hermetic sealing.

The main housing contains two double sided circuit boards (PCB).

B. *Functional Block Diagram / Electronics*

The signal output of the photodiode array is composed of 8 channels. These channels are amplified in transimpedance amplifiers (TIA) and combined to get rid of the DC offsets, which are by factors higher than the desired AC signals. Four of the 8 channels belong to the incremental path as sketched in Fig. 4. After combination, these signals are called SIN and COS. They are A/D converted by a radiation hardened A/D converter with 12 bit resolution and with 2 MHz sampling rate.

The 4 channels belonging to the absolute path are combined to a difference signal (DIFF) and a sum signal (SUM). The SUM signal is compared to a threshold. When the signal is beyond the threshold, the gate signal will toggle. A reference mark is indicated. The centre of the reference mark is determined by processing the DIFF signal, which is A/D converted.

The digitized signals are processed in a Field-Programmable Gate Array (FPGA, Actel RTAX250-S). Position data are transferred to the control system via serial communications based on the LVDS standard. The FPGA sets the gate threshold by pulse width modulation (PWM) and the LED current level by a D/A conversion network. A non-volatile memory is connected to the FPGA to save configuration data and to optionally save position data periodically for a fast initialization.

C. *Optics*

The light source is an AlGaAs/GaAs-LED, which has a small-size emitting aperture. The wavelength is 850 nm. The light is collimated by a lens, made from radiation tolerant glass. The index grating material is fused silica. The photodetector is a Silicon pin-photodiode (PD). LED and PD are placed on ceramics with gold pads for bonding. The ceramics are glued into the optical module, following a passive adjustment. Only the index grating is adjusted actively before fixation with adhesive. These alignment and precision mounting technologies are Tesat developments already qualified and used for more than 10 years for the production of Microwave Hybrid Integrated Circuits (MHIC) and for other opto-electronics like laser heads and receivers used in the Tesat Laser Communication Terminal.

D. *Algorithms*

All A/D converted signals (SIN, COS and DIFF) are low-pass filtered. The incremental signals SIN and COS are offset compensated in order to centre the Lissajous figure. For the

Copyright (c) ICSOS 2012. All Rights Reserved.

interpolation, the Arctan function of the SIN to COS quotient is calculated. A CORDIC (for COordinate Rotation DIgital Computer) algorithm with an interpolation factor of 512 is used. The relative position is determined by counting the periods and adding the result of the interpolation.

The ablated reference marks are about 10 periods of the incremental signal wide. The GATE signal (derived from the SUM signal by a Schmitt trigger) is high during the 10 periods. The DIFF signal has a zero crossing in the middle of the 10 periods. Control algorithms ensure the zero crossing keeps track of the middle of the 10 periods. Therefore, one algorithm trims the offset of the DIFF signal. Another algorithm determines thresholds to adjust the window for zero crossing detection to be one incremental period long. A third algorithm sets the Schmitt trigger threshold.

The number of incremental periods between two adjacent reference marks is counted. In the moment of the sub-divisional angle being zero, the absolute position is derived. If the encoder is in its start-up phase, the reported, up to now relative position will be replaced by the absolute position. Further on, the decoded distance between adjacent reference marks will be used to check the encoder position count for consistence with the absolute position. In case of a discrepancy an error will be signalled.

The incremental signal magnitude ($\sqrt{SIN^2 + COS^2}$, also a result of the CORDIC algorithm) is used to control the signal strength by setting the LED current in an automatic gain control. A control with dead-band is implemented to avoid a steady control jitter.

All algorithms optimize continuously their outputs, executing a permanent calibration. The optimized settings are saved to a non-volatile memory to provide best starting conditions after switch-on.

E. *Data Interface*

In the Laser Communication Terminal, the encoder is located in the Coarse Pointing Assembly, which is exposed to space environment (see Fig. 1). To obtain maximum immunity against electro-magnetic interference, encoder data is transferred digitally from the read-head to the drive system controller which is located in the spacecraft interior. In the encoder read-head, the absolute position is calculated by combining the incremental signal and the reference marks. The absolute position including the encoder status is the answer to each data request. If one datagram is corrupted, the entire set of information will be transferred again within the next cycle. This scheme makes a transmission error correctable, once the next datagram is received. The error is not accumulated.

V. PERFORMANCE AND FUNCTION TESTS

A. *Test Set-up*

To provide the most representative functional testing, the encoder is operated in a test as you fly assembly. That means it is mounted to a motor/bearing assembly, which is identical to the ones, which are part of the Coarse Pointing Assembly (CPA) in a LCT.

As shown in the block diagram Fig. 5 in the lower blue coloured part, the encoder under test and optionally the motor of the bearing unit can be connected to a Motor Drive Electronics (MDE) of a LCT. For the position control a free programmable real time control system is used. The data exchange between the MDE and the embedded control system has a 1 kHz rate.

The jitter performance of the encoder under test is measured by comparing it to a commercial encoder from

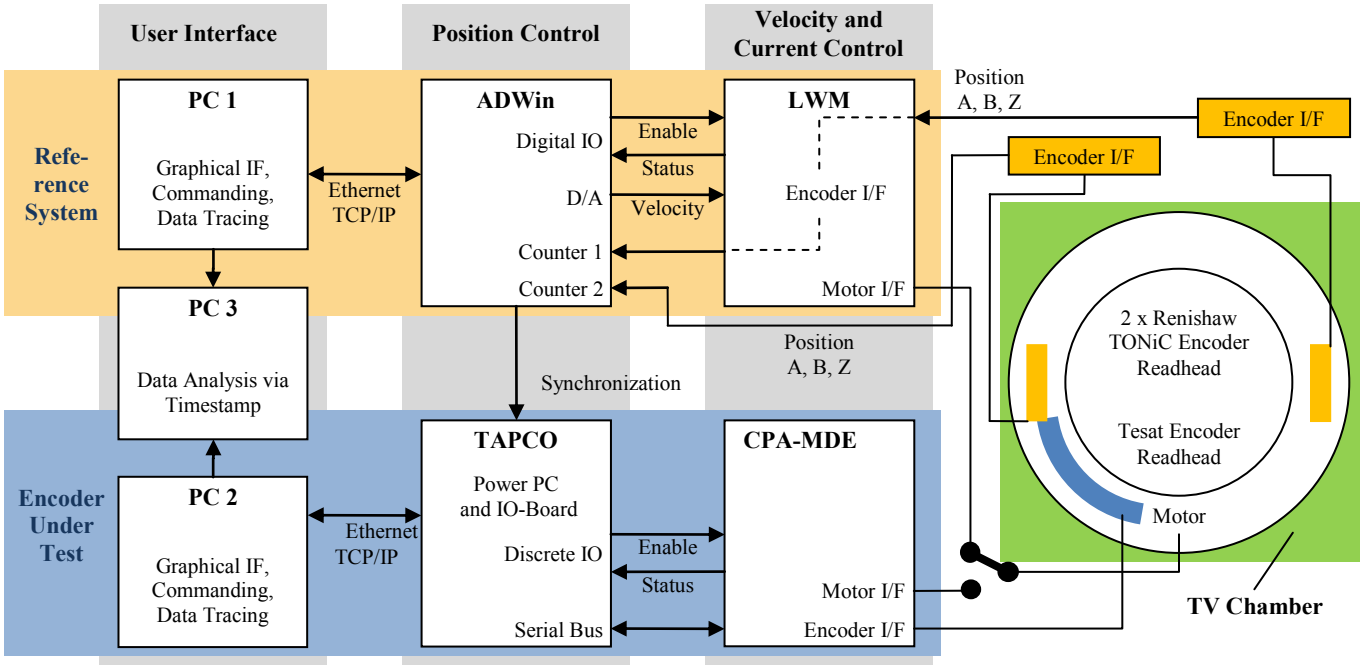

Figure 5. Encoder test set-up block diagram

Copyright (c) ICSOS 2012. All Rights Reserved.

Renishaw, mounted on the same bearing assembly. A totally separated commercial drive and control system (orange coloured in the Fig. 5) is established to move the scale. The commercial encoder is selected to be better in resolution and the position control of the reference system has a higher sampling rate. A second commercial encoder from Renishaw is also mounted to the bearing assembly. So, not only the angular position difference between the encoder under test and the reference encoder, but also between two commercial encoders can be analysed.

The advantages of the chosen set-up are:

- The jitter can be measured up to full speed,
- with full sampling rate and
- over an entire revolution (for example generating 360000 data points for a full rotation at a velocity of 1°/s).
- The set-up is fully suitable for thermal-vacuum tests over the entire temperature range.

The disadvantages are:

- The reference system is not better than the encoder under test with respect to most contributions to the jitter. With a perfect reference system, the measured jitter could be up to two times less than what is measured with the chosen set-up.
- The geometric error of the bearing assembly dominates the position error at low frequencies.
- By comparing two encoders mounted to the same scale, the relationship in phase of the sub-divisional period would lead to constructive or destructive interference, if the interpolation error of both encoders had the same systematic curve. But over the entire revolution, the phase varies by more than 180° by the geometric error, which would reveal interference effects.

B. Jitter Performance

At a velocity of 25°/s, 10°/s and 1°/s, an entire revolution was measured in both the forward and reverse directions. Further measurements were executed at a velocity of 0.1°/s, 0.01°/s and 0.001°/s, of course for a reduced angular range to keep the measurement time and the amount of data acceptable.

The measurements were done at 20°C, +75°C and -35°C.

Four main contributions to the over-all jitter are distinguished, and jitter data are analyzed with respect to these contributions:

- Long range scale error:
  Any long range (> 1° range) scale errors are caused by geometric errors of the bearing system. With the used bearing assembly, this error is about 80 µrad 0-peak in the difference between two encoders. Hence, the maximum absolute error is 40 µrad. This error is repeatable. As it is not a property of the encoder read-head, the large-scale scale error can be ignored as far as possible for the jitter analysis of the encoder read-head.
- Error caused by reference marks:
  If one or two reference marks are in the field of view of the photodiode, an increase in the position error occurs. The basic period is $360°/92 = 3.9°$. This jitter component is about 1 µrad rms at room temperature and increases up to 2 µrad rms at temperature extremes.
- Interpolation or sub-divisional error:
  The interpolation has a non-linear error. The basic period is $360°/27968 = 225$ µrad. The sub-divisional error is about 0.4 µrad rms.
- Random noise:
  Electronic noise and digitizing noise are summarized here. The sampled position is randomly incorrect in the order of 1 increment. The error is in the range of 0.4 µrad rms.

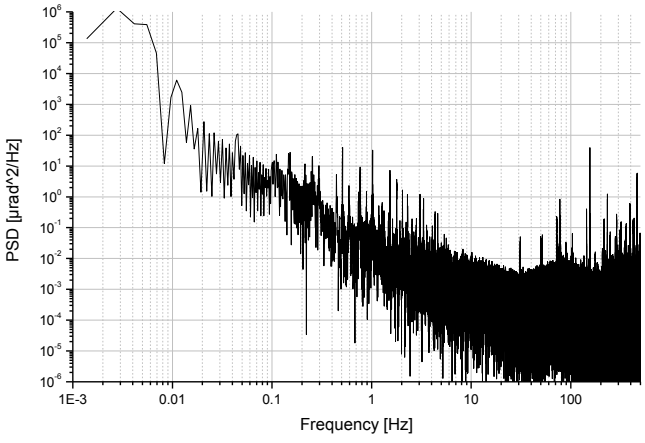

Figure 6. PSD of the position jitter - encoder Tesat relative to Renishaw 1

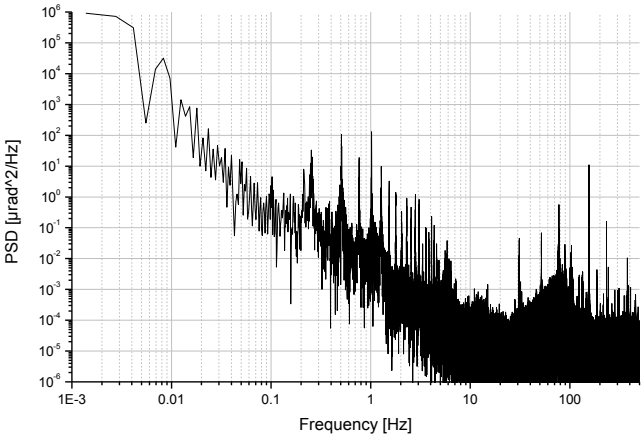

Figure 7. PSD of the position jitter - encoder Renishaw 2 relative to Renishaw 1

Copyright (c) ICSOS 2012. All Rights Reserved.

Best separation of the jitter contributions can be obtained in the frequency domain, using a fast Fourier transformation (FFT). First, the difference between the position data of the encoder under test and the reference encoder (by which the scale is driven) is calculated for each data point.

Following the FFT the power spectral density (PSD) is calculated: The data points of the amplitude spectrum are squared and scaled (by the factor $1/(2 \cdot \Delta f)$ with Δf being the frequency resolution). Fig. 6 is the PSD of the Tesat encoder at 1°/s. For comparison, the PSD of the position difference between two Renishaw encoders is shown in Fig. 7. A significant difference between the Tesat and the Renishaw encoder is the jitter for $f > 100$ Hz. The commercial encoder was selected to have a better resolution leading to less digitizing noise. Concerning all other noise contributions, the Tesat encoder has achieved a similar performance as its commercial standard.

At a velocity of 1°/s, the interpolation error has a fundamental frequency of 77.7 Hz. This peak and harmonics can be seen in Fig. 6. The frequency of the reference mark induced error is 0.256 Hz and harmonics. Also these lines can be seen, but not so accentuated, because the position of every second mark is varied along the scale spreading the frequency.

In order to extract the numerical value of a certain jitter contribution, the PSD is used to calculate the root mean square (RMS) versus the corresponding frequency range: PSD_i be a single PSD frequency component. The formula for the RMS is:

$$\alpha_{\mathrm{rms}}(f_1 \le f \le f_2) = \sqrt{\sum_{i(f_1)}^{i(f_2)} \mathrm{PSD}_i \cdot \Delta f}$$

In Tab. I, the RMS jitter values over a frequency decade are summarized for different test runs. Lowering the velocity from 1°/s to 0.1°/s tends to shift the jitter values by 1 decade to the lower frequency, which is obvious for all contributions having a fix angular period. The error by reference marks is allocated to the jitter over two decades around its fundamental frequency; same is done for the sub-divisional error. The result is recorded in every second line of the table.

Concerning the test results at the velocity 1°/s, the jitter at the frequency range from 10 to 500 Hz, which is allocated to the interpolation error, is about 0.6 µrad rms for the Tesat encoder whereas the value for the commercial encoder is 0.24 µrad rms. There is no difference at the velocity 0.1°/s (in the range 1 to 100 Hz, the jitter is about 0.3 µrad rms for all test runs. As stated before referring to the FFT diagrams, the Tesat encoder has the same amount of sub-divisional error as the commercial encoder, but the high frequency noise is bigger. That can also be clearly seen at the jitter value for 0.1°/s and $f > 100$ Hz (0.05 µrad rms compared to about 0.2 µrad rms).

At the end of the jitter performance section, it is briefly discussed, which jitter performance is relevant for the coarse pointing assembly (CPA) in a LCT. The control bandwidth of the CPA is less than 50 Hz. So, errors above 50 Hz are suppressed. Errors below 1 Hz are allowed to be in the order of a few micro-radians, at 0.1 Hz already in the order of a few 10 micro-radians. The encoder is better. Only the frequency range from 1 to 100 Hz is relevant. There, the result worst case is $\sqrt{0.92^2 + 0.44^2} = 1$ µrad rms for -35°C and 1°/s. This value is acceptable for a LCT. Furthermore, a velocity of 1°/s is an extreme during a LCT acquisition, velocities of 0.1°/s and less are more typical. The jitter at 0.1°/s is below 0.4 µrad rms. That's by far a sufficient performance for the CPA of a LCT,

TABLE I. RMS VALUES OF THE POSITION JITTER VERSUS FREQUENCY RANGE

Model	Velocity	Measured Range	Temperature	Position jitter [µrad rms] in the frequency band:					
				0.001 Hz ≤ f < 0.01 Hz	0.01 Hz ≤ f < 0.1 Hz	0.1 Hz ≤ f < 1 Hz	1 Hz ≤ f < 10 Hz	10 Hz ≤ f < 100 Hz	100 Hz ≤ f ≤ 500 Hz
Ref 2 - Ref 1	1°/s	360°	20°C	52.53	3.91	0.89	0.7	0.14	0.19
						RME: 1.13		SDE: 0.24	
Tesat - Ref 1	1°/s	360°	20°C	56.07	4.2	0.95	0.49	0.33	0.55
						RME: 1.07		SDE: 0.64	
Tesat - Ref 1	1°/s	360°	+75°C	50.00	2.82	1.84	0.79	0.37	0.46
						RME: 2.00		SDE: 0.59	
Tesat - Ref 1	1°/s	360°	-35°C	58.57	4.31	1.34	0.92	0.44	0.47
						RME: 1.63		SDE: 0.64	
Ref 2 - Ref 1	0.1°/s	20°	20°C	6.77	0.88	0.78	0.15	0.22	0.05
					RME: 1.18		SDE: 0.27		
Tesat - Ref 1	0.1°/s	20°	20°C	9.90	0.91	0.29	0.11	0.23	0.26
					RME: 0.96		SDE: 0.25		
Tesat - Ref 1	0.1°/s	20°	+75°C	8.12	2.04	0.86	0.15	0.28	0.21
					RME: 2.21		SDE: 0.32		
Tesat - Ref 1	0.1°/s	20°	-35°C	10.07	1.33	0.78	0.16	0.31	0.19
					RME: 1.54		SDE: 0.35		

RME: Jitter allocated to the Reference Marks induced Error

SDE: Jitter allocated to the Sub-Divisional Error

Copyright (c) ICSOS 2012. All Rights Reserved.

even more taking into account the jitter contribution by the test set-up.

C. Functional Tests

All functional tests were passed. The encoder continuously delivers various housekeeping data, which are used to evaluate the function and performance of the control and compensation algorithms. One housekeeping parameter is the LED current. As the amplitude of the A/D converted signal is kept constant by an automatic gain control, the LED current is a measure for the success of the encoder alignment during production and installation. The LED current is below the budgeted value over the entire temperature range. 18% of the maximum (already derated) LED current are used at 20°C. The value is increased to 37% at +75°C and at worst case impact of the reference marks. Life-time effects can be compensated with ample safety margin.

After start-up, the encoder is relative. It is moved over a few reference marks, meanwhile the control algorithms find optimal settings. The absolute position is determined, and the optimized configuration is saved to memory as start-up configuration for the next power-up cycle.

The mass of the encoder is about 250 g without cable assembly. The power consumption is typical < 1 W, whereas the specification allows a power consumption up to 3 W.

VI. Environmenatl Tests and Qualification

A. Electronic Parts

All used electronic parts are HiRel components which are purchased and qualified by Tesat's Part Agency.

Very few of Renishaw's commercial optoelectronic key components are used, and these were sourced in batches: the LED and the photodiode. The LED comprises AlGaAs/GaAs technology which is well known to be robust with regard to high temperatures and radiation. The silicon photodiode makes use of a pin structure where the same applies. Sourced LED and photodiode batches underwent lot qualification tests according to Tesat standards. In Fig. 8 the evaluation test flow for the LED is shown, comprising 70 pieces in total. The test flow for the photodiode is similar, see Fig. 9. 120 pieces were used.

Concerning radiation, samples were irradiated with protons. Fluences were chosen such that test levels exceed application values equivalent to 15 years Geo orbit by a factor of ~10. The LED output power typically decreased by ~4%. Even for these excess fluence levels, this reduction is well within the optical budget. The dark current of the photodiodes increased from pA to nA levels. These are approximately three orders of magnitude lower than operational values on µA level caused by photocurrents and hence do not influence the precision of the encoder.

Both LED as well as photodiode passed temperature cycling according to MIL-STD-750 (Method 1051, Condition C), moisture testing according to MIL-STD-750 (Method 1021), a Construction Analysis and ESD testing without identifying weaknesses. The LED was subjected to an Operating Life Test at high temperatures, the photodiode to High Temperature Reverse Bias (HTRB) Life Test, both for 2000 hours. All samples passed the tests without findings.

B. FPGA

The code in the FPGA was developed according to the standard ECSS-Q-ST-60-02C. Emphasis was placed on the verification of the code (written as VHDL, VHSIC hardware

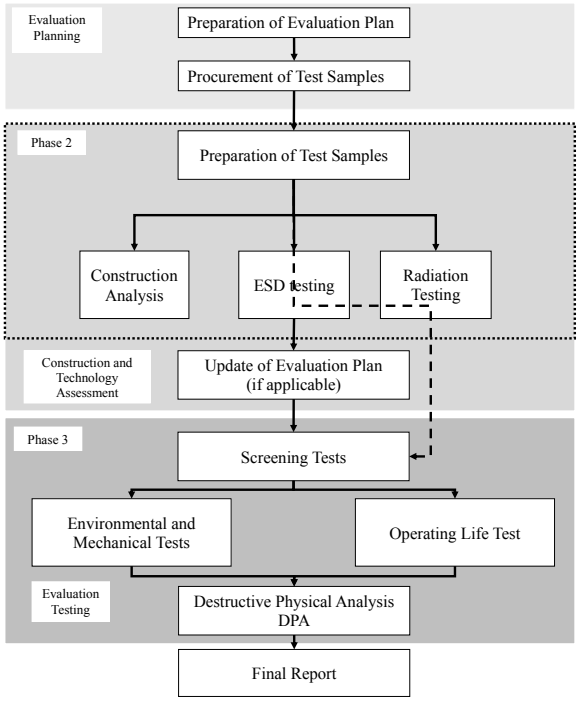

Figure 8. Evaluation test flow LED

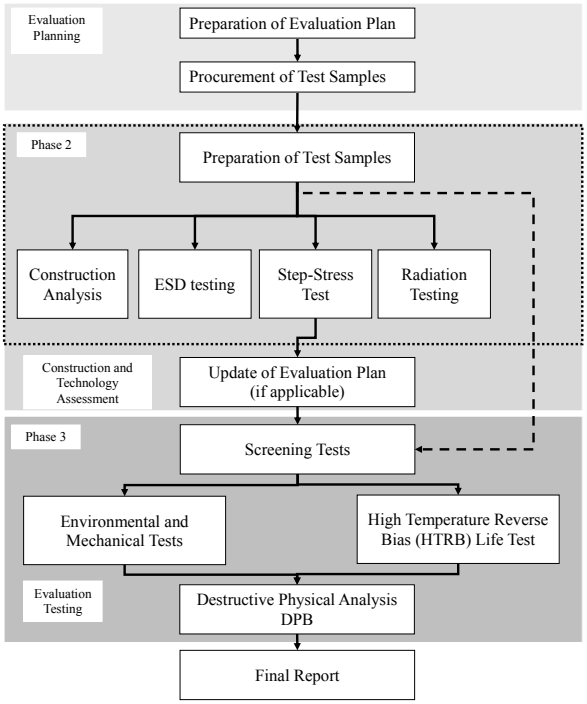

Figure 9. Evaluation test flow Photodiode

Copyright (c) ICSOS 2012. All Rights Reserved.

description language). In order to stimulate the code under test, the scale movement was simulated by a separated VHDL module.

For the validation phase, a test board was manufactured comprising the FPGA and peripheral devices (e.g. the memory device). Additionally, a combined pattern generator / logic analyzer was connected for stimulation of FPGA inputs and simultaneous monitoring of all input/output pins. Timing was uncritical, all tests were passed.

C. *Optical Module*

The optical module is treated as a self-contained sub-assembly with its own specification, evaluation and qualification approach, which is based upon standards (ESA-PSS-612) applicable on MHIC (Microwave Hybrid Integrated Circuit) modules.

Most of the processes used in the optical module were already qualified Tesat processes, before the encoder development was started, and have heritage e.g. in laser head modules. For some items, a dedicated evaluation program was successfully executed, namely for the attachment of the index grating, for the geometric accuracy of the collimator sub-assembly and for the custom-designed package. For the latter, a Destructive Physical Analysis (DPA) was performed.

All produced optical modules are submitted to a screening and electrical performance testing. Some samples are allocated to evaluation, comprising:

- 500 thermal cycles (-40°C to +100°C)
- Mechanical shock (according MIL-STD-883,Method 2002, Condition C)
- Moisture resistance testing (85°C / 85% humidity)

Further on, other samples are allocated to Circuit Type Approval (CTA) and Lot Acceptance Test (LAT), comprising:

- Electrical testing at -40°C, 20°C and +80°C
- Active lifetest 2000 h at 125°C (according MIL-STD-883, Method 1015), repetition of the performance test afterwards
- External visual inspection, X-ray inspection
- Solderability, lead integrity
- Geometry measurement
- Decapsulation
- Internal visual inspection, Scanning Electron Microscope (SEM) inspection
- Wire pull test, ball shear test, substrate attach strength, die shear strength

All performance tests, evaluation tests, CTA and LAT tests were successfully executed.

D. *Encoder*

The flow of the encoder test campaign is shown in Tab. II. The results of the function and performance tests were presented in chapter V. No change in performance following an environmental test was measured.

TABLE II. ENCODER TEST FLOW

No.	Abbre-viation	Test	FM	QM
1	IFT	Initial Functional/performance Test	X	X
2	VT	Vibration Test	X*1)	X*2)
3	PVT	Post Vibration functional Test	X	X
4	TVT	Thermal Vacuum Test	X*3)	X*4)
5	FT	Functional Test	X	X
6	EMC	Electro-Magnetic Compatibility Test	X*5)	X
7	ST	Shock Test		X
8	FFT	Final Functional/performance Test	X	X

X Test to be performed
*1) No sine vibration, random vibration with acceptance level, no shock
*2) Sine and random vibration with qualification level, no shock
*3) Including 4 non-op cycles over acceptance temperature range
*4) Including 8 non-op cycles over qualification temperature range
*5) EMC test can be omitted, if EMC requirements are met by QM unit

Vibration was tested with the specified level of 24.7 g rms. Following the resonance search, the load run was executed with the spectrum at the encoder mounting interface as shown in Fig. 11. The excitation was in x-direction as sketched in Fig. 10. The answer spectrum as shown in Fig. 12 was measured at the top of the optical module (see “RMP-1X Sensor” in Fig. 10). The dominant resonance peak is as calculated in the mechanical analysis. This peak is caused by a rotational mode around an axis, which is parallel to the long axis of the mounting interface.

For the thermal vacuum (TV) tests, the same set-up as for the performance tests was used. Fig. 13 is a photo of the bearing assembly, equipped with one Tesat and two Renishaw encoders and mounted to the plate, which is cooled or heated in the TV chamber. Fig. 14 is a temperature chart of the complete TV test campaign. The red trace is related to a sensor on the plate. The other traces are related to sensors on the encoder

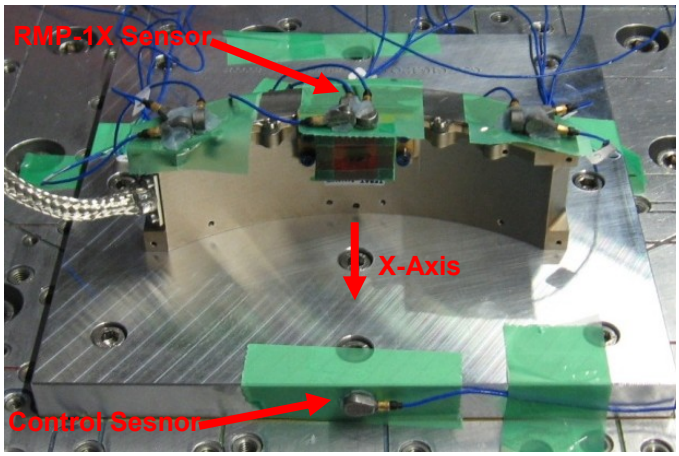

Figure 10. Encoder in vibration test configuration

Copyright (c) ICSOS 2012. All Rights Reserved.

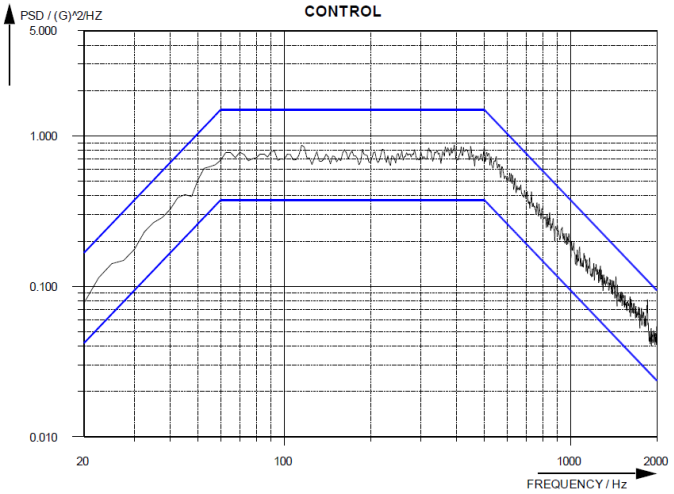

Figure 11. Vibration control spectrum in x-axis at mounting interface

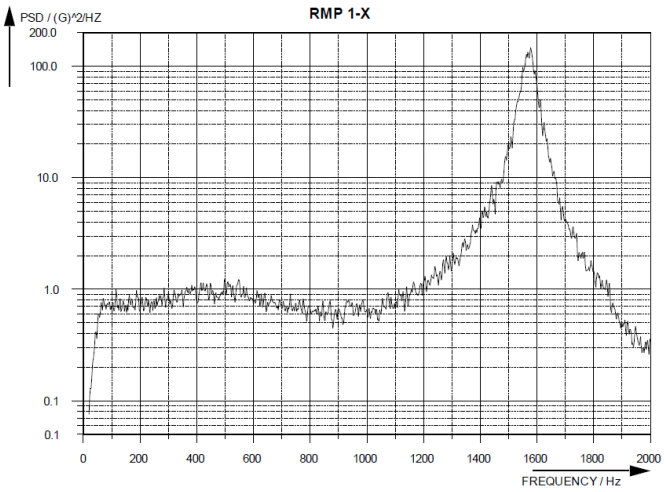

Figure 12. Vibration spectrum in x-axis at top of optic module housing

housing. Five performance and switch-on test blocks were executed: at 20°C after installation of the set-up (A1 in Fig. 14), at -35°C and +75°C, each before (C1, H1) and after passive cycling (C2, H2). The encoder was operated during the first temperature cycle (between C1 and H1), four passive cycles followed. For a Qualification Model (QM), the number of passive cycles will be doubled. The temperature range will be extended to -40° to +80°C. The LED current is increased at temperature maxima, as the automatic gain control keeps the incremental signal level constant. Without control, the level would decrease, caused by both reduction in efficiency and a shift in the LED wavelength. The LED current rise over temperature is well inside the LED current budget. Encoder performance and function were within specification over the entire temperature range.

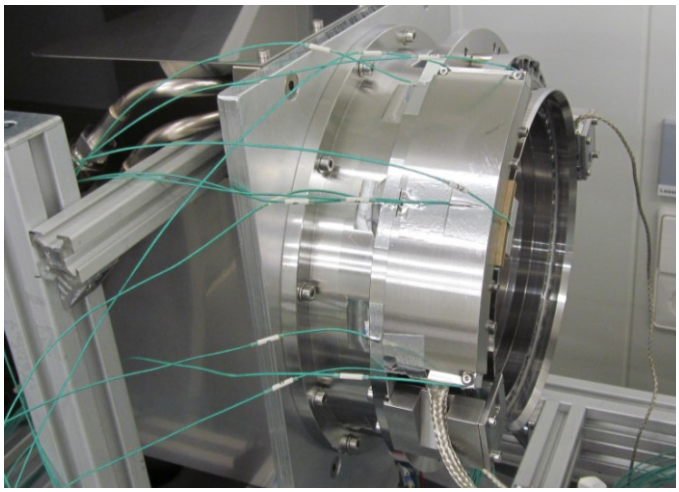

Figure 13. Encoder mounted for thermal vacuum test

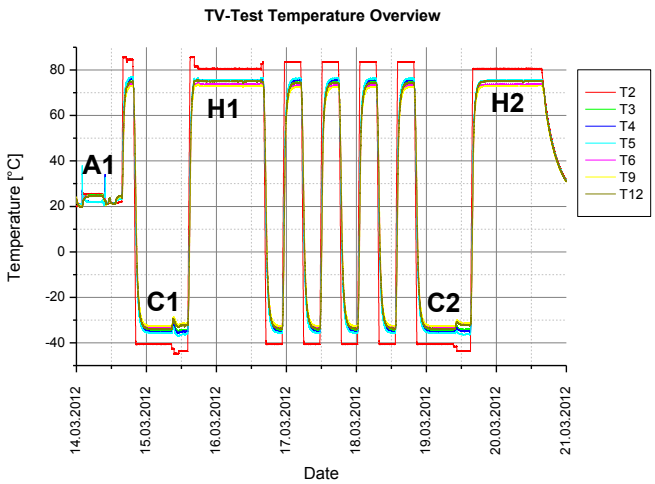

Figure 14. Temperature during thermal vacuum test

Concerning electro-magnetic compatibility tests (EMC), radiated emission was measured to be below the specified limit, which is set 10 dB below MIL-STD-461/462 E standard.

A complete EMC test (including radiated and conducted susceptibility and radiated emission), a TV test with qualification temperature range, a vibration test with QM duration and a shock test are subjected to the on-going tests with an encoder engineering qualification model (EQM).

VII. Summary, Outlook and Acknowledgment

Together with Renishaw, Tesat has successfully developed and tested a space qualified optical encoder. While it was tailored to the operation in a LCT under harsh environmental conditions outside the spacecraft in a GEO orbit, it can be used as well for many other applications in high precision, long life space instruments.

For applications where mass and volume of the read-head are crucial, a separation of the optical module and the signal processing electronics is a straightforward modification, as the optical module is already a self-contained sub-assembly.

The funding support of the German Space Center, DLR is gratefully acknowledged. The development of the encoder was supported by the DLR under contract number 50 YH 0932.

Copyright (c) ICSOS 2012. All Rights Reserved.